JT9D Performance Deterioration Results from a Simulated Aerodynamic Load Test

Edward G. Stakolich*
NASA Lewis Research Center, Cleveland, Ohio
and
William J. Stromberg†
Pratt & Whitney Aircraft Group, United Technologies Corporation, East Hartford, Connecticut

This paper presents the results of testing to identify the effects of simulated aerodynamic flight loads on JT9D engine performance. The test results were also used to refine previous analytical studies on the impact of aerodynamic flight loads on performance losses. To accomplish these objectives, a JT9D-7AH engine was assembled with average production clearances and new seals, as well as extensive instrumentation to monitor engine performance, case temperatures, and blade-tip clearance changes. A special loading device was designed and constructed to permit application of known moments and shear forces to the engine by the use of cables placed around the flight inlet. Upon completion of the test program, the test engine was disassembled, and the condition of gas path parts and final clearances were documented. The test results indicate that the engine lost 1.1% in thrust specific fuel consumption, as measured under sea-level static conditions, owing to increased operating clearances caused by simulated flight loads. This compares with the 0.9% predicted by the analytical model and previous study efforts.

Introduction

THE high cost of fuel for aircraft gas turbine engines has resulted in a concerted effort to minimize performance deterioration during the life of an engine. In response to the need for better fuel efficiency, NASA initiated the Aircraft Energy Efficiency (ACEE) Program in 1975. An element of this program, engine diagnostics, managed by the Lewis Research Center investigated the causes and extent of performance deterioration of high-bypass ratio turbofan engines. As part of this program, the Commercial Products Division of the Pratt & Whitney Aircraft Group was awarded a contract to determine the extent and causes of performance deterioration of their JT9D engine. Investigation of historical data[1] on the JT9D engine, along with performance data obtained from 32 JT9D-7A engines in the Pan American World Airway's fleet of Boeing 747 SP aircraft,[2] have indicated that a performance loss of 0.7% cruise specific fuel consumption (SFC) occurs in the first few flights of the aircraft. A substantial portion of this loss occurs during flight acceptance testing of the airplane prior to its delivery to the airline and therefore is not part of revenue service deterioration. This deterioration is caused by increased operating clearances between rotating fan, compressor, and turbine blade tips and their outer air seals. Engine case and rotor deformations result from aerodynamic loads on the engine inlet cowl and inertia loads on the engine which occur during flight. These deformations cause rubbing of the rotating blade tips on their outer air seals (Fig. 1) which produces the increased clearances reducing the efficiency of the engine.

The Pratt & Whitney Aircraft Group assisted by the Boeing Commercial Airplane Co. has also developed an analytical technique to predict the effects of aircraft flight loads on the performance deterioration of the JT9D engine.[3] This analysis utilizes a NASTRAN finite-element model (Fig. 2) of the JT9D engine in a 747 aircraft nacelle to relate inlet aerodynamic loads, propulsion system inertia loads, and engine thrust and thermal loads to engine structural deformations. The analysis technique converts these deformations to permanent blade-tip clearance changes and calculates the associated performance loss.

An aerodynamic load simulation test[4] has been conducted by P&WA in their x-ray test facility to determine the effect of these loads on the performance deterioration of the JT9D engine. The objective of this test program was to determine whether the short-term loss in performance was caused by these aerodynamic loads, or by thrust/thermal loads, or by a combination of both. Blade-tip clearance changes were measured with laser proximity probes and x-ray techniques. Using the P&WA component design system, engine and module performance losses were determined from expanded performance instrumentation and the results of an analytical teardown of the engine after testing. This paper describes this test program, presents results, and compares these results with the performance deterioration models developed from actual in-service engine data and the NASTRAN analytical model predictions.

Test and Facility Hardware

Engine

The engine used in the test program (JT9D-7AH model) was built from serviceable modules of flight quality. The modules were assembled with new inner and outer air seals, and all gas path seal clearances were set to production blueprint limits. During assembly, all gas path clearances were measured and recorded. Certain engine cases were experimental in order to accommodate the installation of experimental instrumentation. For the test program, the engine was installed in a 747-200 nacelle with a flight inlet to simulate the structural load paths which occur in the flight installation.

Test Facility

The test was conducted in the P&WA production radiographic test stand (Fig. 3). This stand was designed for

Presented as Paper 81-1588 at the AIAA/SAE/ASME 17th Joint Propulsion Conference, Colorado Springs, Colo., July 27-29, 1981; submitted Sept. 4, 1981; revision received Aug. 25, 1982.

*Aerospace Engineer, Facilities and Mechanical GSE Section, Launch Vehicles Division.

†Senior Staff Engineer, Advanced Resource Planning, Commercial Engineering.

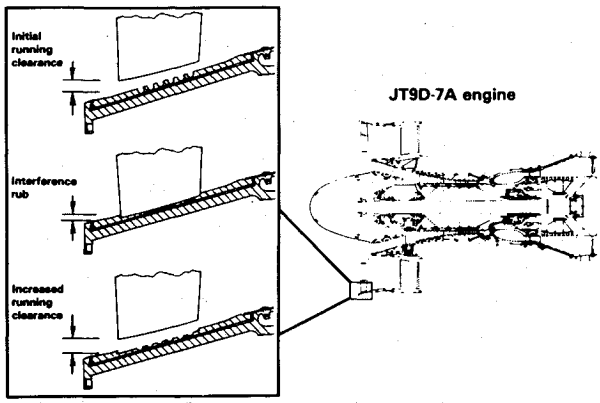

Fig. 1 Effect of aerodynamic flight loads on fan blade-tip clearance.

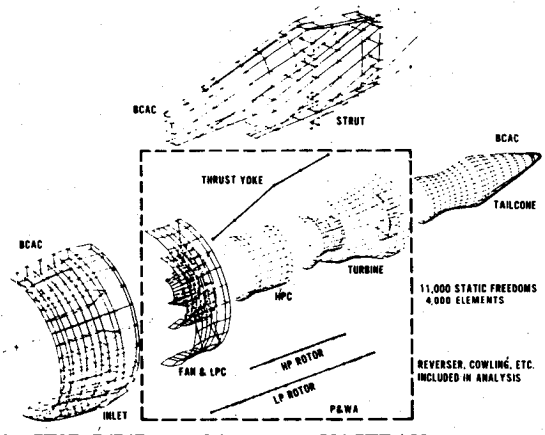

Fig. 2 JT9D-7/747 propulsion system NASTRAN structural model.

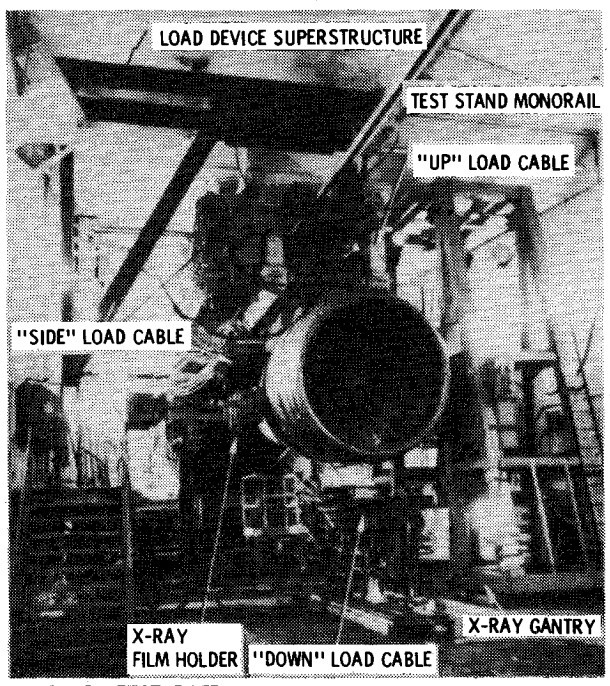

Fig. 3 JT9D-7AH test engine prepared for approach load.

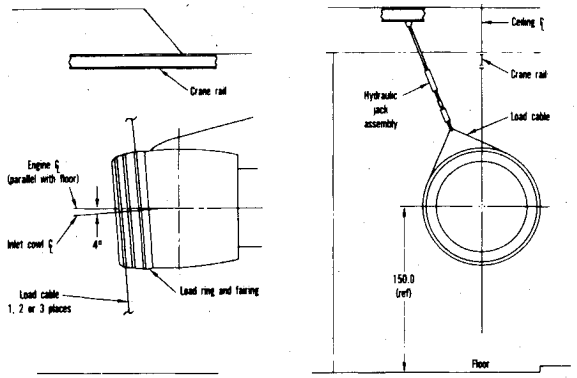

Fig. 4 Engine cowl load test setup.

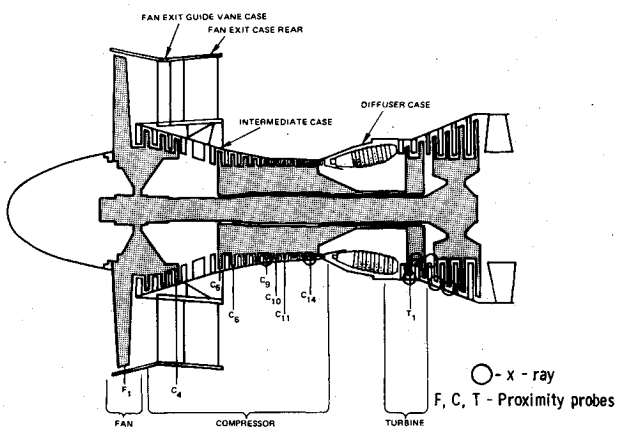

Fig. 5 Proximity probe and x-ray locations.

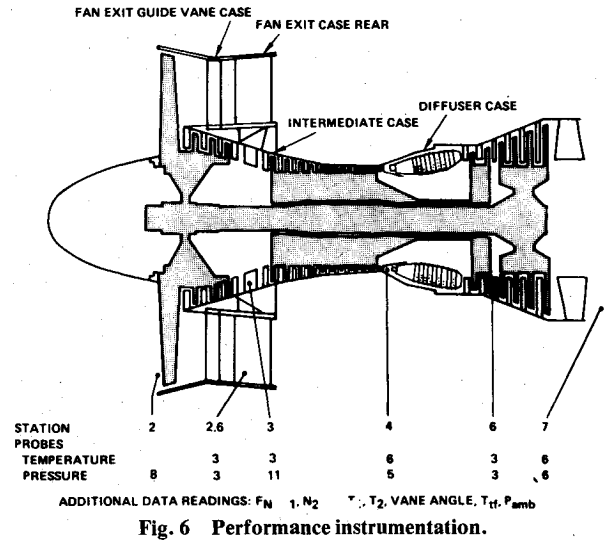

Fig. 6 Performance instrumentation.

sea-level testing of large high-bypass gas turbine engines with airflow rates up to 3000 lb/s. The stand is equipped with a fully automatic production test data acquisition and control (APTDAC) system which programs the engine test, including the performance of such operations as starting, ignition, bleed valve checks, trimming, and limit checks.

A unique feature of this facility is its radiographic capability, which was utilized for engine internal clearance measurements during the test program. The system is capable of recording internal clearances during engine steady-state and transient operations as well as static conditions.

Loading Device

The test stand was modified for the installation of a loading device for the simulation of inlet aerodynamic loads. Loading combinations were applied at three inlet cowl rib locations through wire cables wrapped around the inlet. The proper combination of load cables pulling at the required angles produced forces and moments on the engine equivalent to the aerodynamic flight load.

The design developed by P&WA and Boeing is shown in Fig. 4. A loading strap is located at each of the three forward inlet cowl ribs. Each strap is in contact with a rubber strip bonded around the circumference of the cowl. Bonded to each strip is a machined steel ring notched to accept a wire cable, each end of which terminates at a hydraulic jack assembly. The machined steel rings are submerged in a polyurethane sheet to provide a smooth aerodynamic surface to prevent turbulent air from being generated and drawn into the inlet from the region of the loading fixture.

Each hydraulic jack assembly contains a jack, a load cell to measure applied load, and an overload protection device which allows the engine to move during transients or an engine stall. The hydraulic jack assemblies are supported by the base and supporting structure.

Instrumentation

Blade-Tip Clearance Measurements

Laser proximity probes were used to obtain clearance changes between the fan, compressor, and high-pressure turbine blade tips and their outer air seals during engine operation. Nine engine stages were instrumented (Fig. 5) with four probes per stage located circumferentially around each engine case. The actual angular location of each probe was governed by local access to bleed ports to facilitate routing of fiber optic bundles through outer engine case walls. Seven areas in the high-pressure compressor (HPC), high-pressure turbine (HPT), and low-pressure turbine (LPT) were x-rayed to obtain both inner and outer air seal clearances (Fig. 5). The low-pressure turbine with shrouded blade tips produced good quality x-ray photographs from which blade-tip clearances were measured. X-ray photographs of the high-pressure compressor and high-pressure turbine were used as backup to the more accurate proximity probe data for determining blade-tip clearance changes.

Engine Performance Measurements

Two data acquisition systems were utilized to obtain engine performance measurements during the test program. The primary system, the APTDAC system is normally used for production testing. Measurements are acquired by the system and converted to engineering units. The converted data are used to calculate the required performance parameters, and the results are checked to determine out-of-limit conditions. The system is designed to perform real-time data acquisition and display the output results on a CRT and a line printer.

Owing to the large number of parameters being measured, a portable, High Accuracy Pressure and Temperature Data Acquisition System (HAPTS) was used to support the production data system. The HAPTS has the capacity to record up to 600-bipolar-mV inputs and 192 pressure inputs on four 48-port scanivalved transducers.

In order to assess module performance deterioration from the test, pressures and temperatures in addition to normal production data were recorded during the test program. The location of the performance instrumentation is shown in Fig. 6.

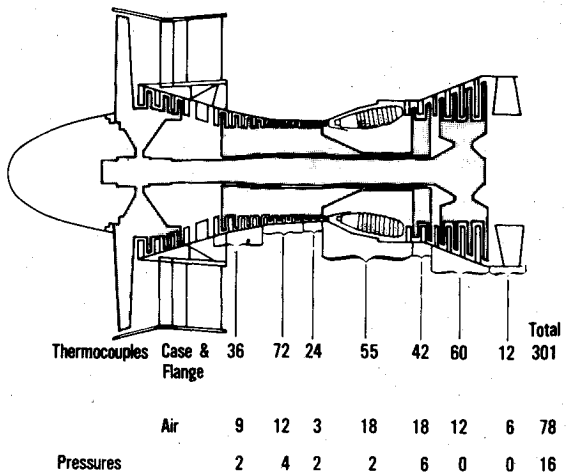

Fig. 7 Thermal load measurements; thermocouple and pressure instrumentation locations.

Engine Case Thermal Measurements

The engine cases were instrumented with thermocouples to measure case temperature variation both axially and circumferentially to correlate axisymmetric and asymmetric thermal closures. Nacelle air temperature and pressure were also measured to determine heat-transfer characteristics within the nacelle environment. The locations of this instrumentation are shown in Fig. 7.

The locations of case, flange, and air thermocouples were chosen to determine the impact of engine case metal temperature on adjacent blade-tip clearance and to determine the effect of engine external components on the engine's thermal environment.

Test Program

This test program was initiated to provide a better understanding of the relationship between steady-state inlet air loads and engine running clearances, as well as the effect of these air loads on engine performance deterioration. To achieve these objectives, a test program was developed using a new JT9D-7AH engine in a 747-200 nacelle (as defined in the Test and Facility Hardware section of this paper). The engine was ground tested under simulated aerodynamic flight loads during which blade-tip clearance, engine performance, and thermal data were obtained. The engine was torn down at the completion of the program to measure physical deterioration.

Four flight conditions from the Boeing 747 aircraft flight acceptance test were selected for simulation in this program. These were takeoff, late climb/early cruise, maximum dynamic pressure, and approach. Aerodynamic loads on the inlet cowl at each of these flight conditions were simulated using the strap-type loading device described earlier. The loads were developed by Boeing from analytical and test (wind tunnel and flight) data. These loads were applied to the engine in both a static and a running condition.

Table 1 Simulated flight loadings

Flight condition	Approximate thrust, lb	Moment applied to "A" flange during static loads testing,[a] in.-lb	Moment applied to "A" flange during combined loads testing,[b] %
Approach	6700	190,670	50,75,100,150
Late climb/early cruise	29,000	65,881	50,100,120,140
Maximum dynamic pressure	43,000	232,234	50,75,100,150
Takeoff	46,000	356,288	25,50,75,100

[a] Typical revenue service load. [b] Percent of typical revenue service load.

The testing was divided into three major parts to satisfy the objectives of the program. The first investigated the effects of thermal and thrust loads on engine running clearances. The second determined the static (nonrunning) engine response to the applied inlet air loads. The third explored the effect of combined thermal, thrust and inlet air loads on the engine. The test program was sequenced so that wear produced by the smaller loads was not disguised by that produced by larger loads. Performance was monitored continuously to determine which test conditions resulted in performance loss. A more detailed description of the testing follows.

Baseline Clearances and Performance Calibration

After the engine was installed in the test stand, but prior to any engine operation, a series of x rays was taken of selected inner and outer gas path seals throughout the engine. These x-rays were taken both at the top (0 deg) and bottom (180 deg) of the engine and served as the baseline for any seal wear that might occur during testing. These measurements also served as a calibration of the x-ray system against clearance measurements taken during the analytical build of the engine.

The engine was then motored with the starter to obtain proximity probe clearance measurements at the nine instrumented engine stages. These measurements were compared to those taken during the analytical build of the engine to arrive at a reliable set of clearances prior to the start of testing. These clearances were then used as baseline measurements to determine blade-tip clearance changes during the test program.

To determine the baseline engine and module performance levels, a baseline calibration consisting of 12 equally spaced power settings was conducted. Each power setting was stabilized for 7 min before recording engine and module performance data, engine case environmental data, and engine running clearance. Throughout the test program, when a significant performance change was indicated, this 12-point calibration run was repeated.

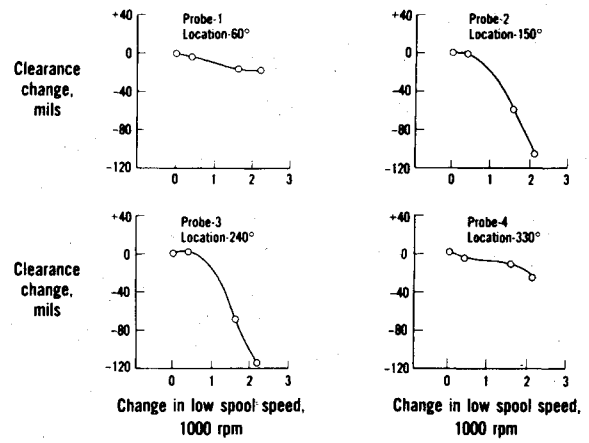

Fig. 8 Fan clearance changes (from ground idle) due to thermal loads—proximity probe data.

Thrust and Thermal Load Effects

The objective of this portion of the test program was to determine the effects of thrust and thermal loads only on engine blade-tip clearances and to determine whether any performance loss occurred owing to these loads. The thrust/thermal environment for each of the four flight conditions from the 747 aircraft acceptance test was simulated. Since the test stand is at sea-level static conditions, not all of the significant engine parameters could be simulated for the altitude flight conditions. The discharge temperature of the high-pressure compressor, T_{T4}, was used as the controlling parameter in setting engine power. To simulate the

Table 2 Predicted axisymmetric clearance changes vs power due to thrust and thermal loads (clearance change in mils from ground idle)

Module/stage	Ground idle	Approach	Climb/ cruise	Maximum Q	Takeoff
Fan	0	−5	−28	−69	−72
LPC					
2	0	−4	−25	−36	−40
3	0	−2	−11	−17	−19
4	0	−3	−20	−30	−33
HPC					
5	0	−5	−16	−21	−22
6	0	−5	−18	−23	−25
7	0	−4	−16	−20	−21
8	0	−5	−18	−23	−25
9	0	−6	−14	−19	−20
10	0	−3	−10	−14	−14
11	0	−2	−8	−10	−10
12	0	−1	+1	+3	+3
13	0	−3	−8	−12	−12
14	0	−2	−8	−11	−11
15	0	−3	−10	−13	−14
HPT					
1	0	−6	−21	−24	−25
2	0	−9	−26	−30	−32
LPT					
3	0	−11	−9	−5	−1
4	0	−2	−25	−22	−21
5	0	−2	−36	−42	−46
6	0	−2	−34	−41	−45
Relative rotor speed changes:					
N_1, rpm	0	341	1596	2100	2234
N_2, rpm	0	605	1848	2295	2390

Table 3 Clearance changes due to 100% aerodynamic loads applied to the static engine (based on proximity probe data)

Module/stage	Probe	Circumferential location (rear view), deg	Flight condition, clearance changes, in. Approach	Climb/cruise	Maximum Q	Takeoff
Fan	1	60	+0.029	+0.016	−0.011	...
1	2	150	−0.019	−0.006	+0.019	−0.041
	3	240	−0.040	−0.009	0	−0.065
	4	330	...	...	−0.025	...
LPC	5	77	+0.003	+0.003	+0.003	+0.003
4						
HPC	9	96	+0.001	...	...	...
5	11	276	0	0	−0.001	+0.001
	12	349	0	+0.001	...	+0.001
HPC	17	47	+0.001	+0.003	+0.006	0
9	18	133	0	−0.001	−0.003	+0.002
	19	191				
	20	313	+0.003	−0.001	+0.005	+0.001
HPC	21	60	−0.007	−0.003	...	...
10	22	135	−0.002	+0.010	−0.007	0
	23	192	+0.003	+0.002	−0.001	+0.005
	24	315	+0.001	0	+0.004	−0.001
HPC	25	75	−0.006	−0.004	−0.005	−0.007
11	26	165	0	−0.001	−0.007	+0.001
	27	248	0	−0.003	−0.005	+0.001
	28	345	−0.003	−0.001	+0.003	−0.005
HPC	30	121	−0.002	−0.003	−0.006	0
14						
HPT	33	650	+0.006	+0.003	+0.006	+0.005
1	34	150	+0.006	+0.004	+0.011	+0.003
	35	230	...	+0.006	...	...
	36	330	...	+0.012	+0.004	...

altitude power setting then, T_{T4} was set as close to the altitude value as possible without exceeding engine thrust, temperature, and rotor speed limits. Approximate thrust values are shown in Table 1.

In addition to the four flight condition test points, clearance and thermal data were also recorded during the baseline performance calibration test to obtain thermal closures between blade tips and outer seals over a wide range of operating conditions. During each test sequence, proximity probe, engine case thermocouple, and performance data were recorded simultaneously. X-ray photographs of the low turbine area were also obtained at each test point.

Static Load Effects

Simulated aerodynamic loads as shown in Table 1 were applied to the engine in a nonrunning (static) condition using the loading device described previously. Additional loadings of 50% takeoff, pure vertical, and pure horizontal were also applied.

During each of these loading conditions, the engine was motored with the starter to obtain proximity probe data on the nine engine stages. X rays of the low turbine area were also obtained at each test load. All strap load values were recorded during the test.

Combined Loads Effect—Thermal, Thrust, and Aerodynamic

The objective of this part of the test program was to determine engine blade-tip clearance changes that occur under simulated flight conditions from the combined effects of thermal, thrust, and aerodynamic flight loads. A total of 16 combined load conditions were tested, including four load levels at each of the four selected flight conditions to be simulated, as shown on Table 1. The 100% load for each condition represents a typical revenue service flight load. The maximum load for each condition was chosen not to exceed the 1/5000-flight load level and is less than the engine/nacelle structural limit values so that no damage to engine cases or nacelle cowls would be expected.

A typical test sequence for this part of the program consisted of bringing the engine up to the desired power level and stabilizing for approximately 7 min, applying the required simulated aerodynamic load to the inlet through the loading device, and then recording proximity probe blade-tip clearance data as well as thermal and performance data. X-ray photographs were also taken.

Transient Tests

At the end of the test program, two severe transient power conditions were run with no aerodynamic load simulation. The first consisted of a 10-min stabilization at full takeoff thrust, followed by a rapid deceleration to ground idle, and another 10-min stabilization. The second transient performed separately from the first was a snap acceleration from ground idle to full takeoff thrust after a 10-min stabilization at ground idle. After reaching takeoff thrust, the engine was stabilized at this condition for 10 min. Immediately preceding each transient, proximity probe readings, engine case environment, and performance data were recorded. All pretransient measurements were repeated after the 10-min post-transient stabilization.

Final Performance and Clearance Measurements

At the conclusion of the test program, the 12-point performance calibration was repeated to determine engine and module performance changes. The fan blades were then water washed, and another 12-point calibration was run. A final set

Table 4 Clearance changes due to 100% aerodynamic loads applied to the running engine (based on proximity probe data—from no load power condition)

Module/stage	Probe	Circumferential location (rear view), deg	Flight condition, clearance changes, in. Approach	Climb/cruise	Maximum Q	Takeoff
Fan	1	60	+0.042	+0.016	−0.006	+0.044
1	2	150	−0.022	−0.010	+0.064	−0.040
	3	240	−0.055	−0.008	+0.004	...
	4	330	...	+0.016	−0.070	+0.034
LPC	5	77	...	+0.003	+0.001	...
4						
HPC	9	96	+0.002	+0.001	+0.002	+0.002
5	10	198	...	...	+0.007	...
	11	276	+0.002	+0.001	−0.001	+0.002
	12	349	+0.001	−0.001	...	−0.004
HPC	14	81	...	+0.001	0	+0.005
6	15	215	...	0	+0.004	...
HPC	17	47	−0.006	−0.003	+0.002	−0.016
9	18	133	+0.004	+0.002	−0.003	−0.005
	20	313	−0.002	−0.004	+0.002	−0.006
HPC	21	60	−0.008	−0.003	+0.002	...
10	22	135	−0.001	0	−0.010	−0.002
	23	192	+0.006	0	−0.005	−0.006
	24	315	+0.003	0	+0.004	−0.002
HPC	25	75	−0.006	+0.001	−0.002	−0.007
11	26	165	+0.003	+0.004	−0.005	+0.003
	27	248	+0.009	+0.009	+0.003	+0.004
	28	345	−0.005	0	+0.007	−0.005
HPC	30	121	+0.007	+0.009	...	0
14						
HPT	33	60	+0.013	0	−0.005	−0.002
1	34	150	+0.007	−0.006	+0.005	−0.004
	35	230	...		0	−0.018
	36	330	...	+0.006	−0.006	+0.006

of static blade-tip clearance measurements was made using both x-ray and proximity probe systems. The engine was motored with the starter to obtain the proximity probe readings. In addition to these final two performance calibration runs, a 12-point calibration was also run after the thrust and thermal load sequence and after each of the combined load flight conditions to determine if there were any performance changes caused by these loadings. During the test program, the engine was started 62 times and was run through 86 flight cycles for a total of 147 h.

Engine Analytical Teardown

After completion of the test program, the engine was disassembled for inspection of hardware deterioration resulting from the testing. Blade-tip and outer and inner air seal wear were measured for all stages. Surface roughness was measured on several fan and compressor blades. The turbine vane bow was also measured to determine flow capacity increase. Other measurements were taken throughout the engine to determine whether there was any distortion that could contribute to engine and module performance changes.

Results

Blade-Tip Clearance Changes Due to Thermal Loads

Blade-tip clearance changes which occur during engine operation with no external loads applied are produced by internal engine pressures and temperatures, centrifugal forces on rotating blades, and engine thrust. All of these produce axisymmetric blade-tip clearance changes except thrust, which is reacted off the centerline of the engine. Circumferential thermal gradients around the engine cases can also contribute to nonaxisymmetric clearance changes.

A sample of clearance changes in the fan stage measured with the laser blade-tip proximity probes is shown in Fig. 8. These clearance changes include the nonaxisymmetric contribution of thrust, which is evidenced by a greater clearance change in the lower two quadrants.

Table 2 shows the predicted axisymmetric clearance changes vs engine power which were calculated for each stage from the data derived from this portion of the test program. These clearance changes reflect the (axisymmetric) effects of engine rotor speed, gas path temperatures and pressures, engine case temperatures, and nacelle cavity temperatures and pressures. The circumferential nonuniformities whose effects were removed from these clearances are produced mainly by thrust. Although nonuniform case temperatures exist, they contribute essentially no circumferential variation in clearance. These clearance changes from ground idle through takeoff power show a decrease for the majority of stages which is to be expected.

Blade-Tip Clearance Changes Due to Aerodynamic Loads

Simulated aerodynamic loads were applied to the inlet of the test engine under cold, static conditions to determine the

stiffness characteristics of the JT9D-7A engine. The applied loads simulated the inlet pressure distributions of approach, climb/cruise, maximum dynamic pressure, and takeoff from the Boeing 747 Flight Acceptance Test.

Results of the analysis of the proximity probe data are shown in Table 3. Only the fan experienced significant clearance changes; core clearances usually changed by less than 0.005 in., with 0.012 in. being the maximum change. The clearance changes shown reflect only those due to the applied inlet aerodynamic moment, and thus do not include the effect of engine thrust. The reported clearance changes follow expected trends for the various flight load conditions.

Blade-Tip Clearance Changes Due to Combined Thermal, Thrust, and Aerodynamic Loads

Simulated aerodynamic loads were applied to the inlet of the test engine at stabilized power settings to simulate the combined effects of thermal, thrust, and inlet pressure loads on engine running clearances and performance. The same inlet load conditions applied during static loads testing were used in the combined loads testing. However, the engine was tested over a range of load levels, generally from 50 to 150% of the loads that occur in the Boeing 747/JT9D Flight Acceptance Test. The power levels at which the engine was stabilized were the same as those used in the thermal loads testing.

Combined load results from the analysis of proximity probe data for the 100% loads levels are presented in Table 4. As static test results indicated, only the fan experienced large clearance changes under flight loads. The largest core changes occur in the first high-pressure turbine stage (0.018 in.) and ninth high-pressure compressor stage. Most measured changes in the core, however, were less than 0.005 in. The clearance changes shown reflect engine bending due to both thrust and inlet moments.

Table 5 Blade-tip-measured clearance changes

Module	Stage	Clearance change,[a] in.
Fan	1	0.057
LPC	2	...
	3	0
	4	0.001
HPC	5	0.006
	6	0.012
	7	0.003
	8	0.007
	9	0.002
	10	0.006
	11	0.007
	12	0.007
	13	0.005
	14	0.013
	15	0.014
HPT	1	0.012
	2 front	0.040
	2 rear	0.040
LPT	3 front	0.010
	3 rear	0.016
	4 front	...
	4 rear	...
	5 front	.051
	5 rear	.062
	6 front	.028
	6 rear	.026

[a] Teardown clearance less build clearance.

Transient Test Results

In general, the clearance changes measured during the two transient tests were as expected. The performance calibration test was run after the transient testing revealed no performance loss due to the transient test.

Engine Teardown Results

At the completion of the test program, the engine was disassembled and hardware condition was documented. Measurements taken during the build of the engine were repeated at teardown and included blade-tip clearances, gas path inner air seal clearances, seal land wear locations and depths, airfoil surface roughness, and turbine airfoil flow areas. The hardware condition was then evaluated to determine its impact on engine and module performance.

Clearance changes from engine build measured during teardown are shown in Table 5 for all blade-tip seals. Changes were observed in almost every stage of the engine, with the largest changes being in the fan, the second stage of the high-pressure turbine, and the fifth stage of the low-pressure turbine. In the cold section, these clearance changes were a result of outer air seal wear. In the turbines, they were a result of both blade length loss and gas path outer air seal wear.

Seal land wear patterns observed during the teardown of the test engine are shown in Fig. 9 for the fan. The locations of wear were as expected. Wear in the upper left quadrant was produced by the maximum dynamic pressure air load which pulled the fan case down and to the right. The takeoff air load pulled the fan case up to the right and produced wear in the lower left quadrant of the fan outer air seal.

The volume of seal material worn from each seal land in the test program was determined for the blade-tip seals. Because the seals were new and unworn when the engine was built, the wear volumes were calculated from wear depth, width, and arc length measurements taken at teardown. These wear volumes shown in Table 6 do not include material removed from blade tips in the turbine section of the engine.

Changes in engine performance due to blade-tip clearance changes, airfoil surface roughness increase, and turbine thermal distortion (flow area change) were assessed using the P&WA component design system. The change in performance indicated by a comparison of teardown and build

Table 6 Engine rub-strip wear[a] by stage for test sequence

Module	Stage	Prediction[a]	Test[a]
Fan	1	22.75	23.8
LPC	2	0.63	1.69
	3	1.40	0.20
	4	1.92	...
HPC	5	0.17	0.83
	6	0.38	0.35
	7	0.08	0.16
	8	0.32	...
	9	0.08	0.08
	10	0.07	...
	11	0.28	0.35
	12	0.09	0.07
	13	0.18	0.36
	14	1.24	1.27
	15	0.95	0.96
HPT	1	0.13	0.13
	2	0.39	0.83
LPT	3	0.19	0.19
	4	...	...
	5	0.75	0.73
	6	0.60	0.55

[a] Wear volume (cubic inches).

Table 7 Engine performance loss for various flight load conditions

Test condition	Change in TSFC at constant thrust, %
Baseline	...
After:	
Climb and approach loads	+0.2
Maximum dynamic pressure loads	+0.4
Takeoff loads	+1.4
Snap transients	+1.4
Fan wash (end of program)	+1.3

Table 8 Comparison of component deterioration assessment from teardown results with deterioration assessment from engine data

Component	Change in TSFC estimated from teardown measurements, %	Change in TSFC estimated from engine test data, %
Fan	+0.1	+0.2
LPC	+0.1	+0.2
HPC	+0.4	+0.2
HPT	+0.5	+0.5
LPT	+0.2	+0.2
Total	+1.3	+1.3

measurements was 1.3% thrust specific fuel consumption (TSFC) at sea-level, static, and takeoff conditions. Blade-tip clearance changes accounted for 1.1 of the 1.3% change. The remaining 0.2% was attributed to airfoil surface roughness increase and thermal distortion caused by the experimental nature of the program.

Performance Analysis

The overall engine performance changes and the component performance changes during the course of testing were determined from calibrations of the engine and from the analytical teardown of the engine at the end of the program. Calibrations were run prior to the application of any loads (baseline calibration), after each series of load applications, after a series of snap transients, and, finally, after the fan blades were washed at the end of the program.

The loss in engine performance from the baseline calibration to the end of the program was 1.3% in TSFC. Some performance loss was noted when the simulated climb and approach loads were applied and after the simulated maximum dynamic pressure loads were applied. The major performance loss, however, occurred when the loads which simulated takeoff rotation were applied. Washing the fan blades produced a performance improvement of 0.1%. Table 7 summarizes the engine performance loss throughout the test program.

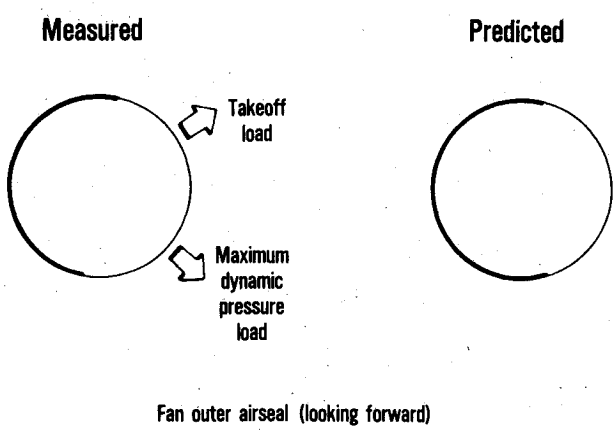

Fig. 9 Predicted vs measured outer seal wear patterns produced by flight loads.

A comparison of the data obtained during the final engine calibration with the baseline calibration was made; and an analysis was conducted to estimate how much each module's degradation contributed to the 1.3% loss in TSFC. Component efficiency and flow capacity changes were expressed as losses in TSFC with the aid of the mathematical simulation of the engine. The assessment of performance loss for each module based on engine teardown results was obtained from measurements of rubs, clearances, and airfoil surface roughness in the compression section of the engine and measurements of rubs, clearances, and airfoil and platform distortion in the turbine section. These measurements and the estimated impact on the performance of each component are summarized in Table 8, which compares the teardown and performance assessment results.

The comparison in Table 8 shows that the high- and low-pressure turbine losses indicated by engine test data agree very well with the teardown results. The total compression section loss indicated by the test data also agrees with that estimated from the teardown measurements. However, the distribution of the loss among the fan, low-pressure compressor (LPC), and high-pressure compressor (HPC) differs somewhat as determined by the two methods. Smaller fan and low-pressure compressor losses and a larger high-pressure compressor loss are indicated by the estimates based on the teardown measurements.

Model Refinements

One of the major objectives of this and previous tasks of the JT9D Engine Diagnostics Program has been the development and refinement of analytical models of JT9D engine performance deterioration. This Simulated Aerodynamic Loads Test Program provided the opportunity to investigate the causes of short-term performance losses and to develop the data with which to modify previous analytical studies and predictions.[3] These analytical predictions, combined with the measured performance losses that occurred during the test program, permitted refinement of the individual models for module as well as engine performance deterioration vs flight cycles developed previously under the JT9D Engine Diagnostics Program.[1,2] In addition, the analytical structural model of the JT9D propulsion system described in the introduction was updated at the conclusion of this test program to better relate the effect of flight loads to engine performance loss.

The updated model was then used to predict the performance loss for this simulated aerodynamic load test program. This predicted loss due to seal wear of +1.1% TSFC shows excellent agreement with the +1.1% measured loss from the test program. Table 6 and Fig. 9 show a comparison of rub strip wear predicted by the model and measured wear from the test program.

Concluding Remarks

The testing and analytical teardown of the JT9D-7AH test engine have significantly improved the understanding of

short-term engine performance deterioration. The overall TSFC change was measured to be +1.1%, which was the result of load induced clearance changes, primarily those resulting from application of the takeoff load. The analytical teardown of the test engine showed clearance changes in all modules, with the major changes occurring in the fan, high-pressure compressor, and high-pressure turbine.

The rub patterns that occurred in the test engine were compared with both analytical model predictions and those rub patterns documented to have occurred in an engine removed from revenue service. In general, the comparison indicates good agreement in most of the engine stages.

The JT9D performance model refined as part of this effort indicates that the flight inlet aerodynamic loads do not substantially contribute to airplane revenue service performance changes, because much of the deterioration caused by these loads occurs during airplane acceptance testing prior to the start of revenue service. This performance increment should not be considered when comparing cruise performance losses with revenue service usage.

Loads testing of the type conducted under this program should be considered on all new engines or engine/nacelle combinations very early in their development. This early testing would provide the longest possible lead time for refining the total propulsion system design. Analytical studies such as those conducted under earlier phases of the Engine Diagnostics Program, and refined under this phase of the program, are considered to be an important element in the preliminary and detailed design of advanced engines and nacelles.

References

[1]Sallee, G.P., "Performance Deterioration Based on Existing (Historical) Data; JT9D Jet Engine Diagnostics Program," PWA-5512,21, Pratt & Whitney Aircraft Group, East Hartford, Conn., April 1978; see also NASA CR-135448, April 1978.

[2]Olsson, W.J. and Sallee, G.P., "Performance Deterioration Based on In-Service Engine Data; JT9D Jet Engine Diagnostics Program," PWA 5512-35, Pratt & Whitney Aircraft Group, East Hartford, Conn., April 1979; see also NASA CR-159525, April 1979.

[3]Jay, A. and Todd, E.S., "Effect of Steady Flight Loads on JT9D-7 Performance Deterioration," PWA-5512-24, Pratt & Whitney Aircraft Group, East Hartford, Conn., June 1978; see also NASA CR-135407, June 1978.

[4]Stromberg, W.J., "Performance Deterioration Based on Simulated Aerodynamic Load Tests, JT9D Jet Engine Diagnostics Program," PWA-5512-75, Pratt & Whitney Aircraft Group, East Hartford, Conn., Feb. 1981; see also NASA CR-165297, Feb. 1981.